Quench Location in the LARP MQXFS1 Prototype

T. Strauss, G. Ambrosio, G. Chlachidze, P. Ferracin, M. Marchevsky, G. Sabbi, S. Stoynev

***Abstract*— The high luminosity upgrade project US LARP/HiLumi has successfully tested the first 1.5 m prototype quadrupole MQXFS1 at Fermilab' Magnet test facility. Several thermal cycles and test programs were performed, with different pre-load configurations. To localize and characterize quenches a quench antenna and voltage taps are used. The quench antenna was placed inside a warm bore of an anti-cryostat centered in the magnet. We varied the length between quench antenna segments from 2.54 cm to 15.24 cm, and shifted the location of the antenna to localize the quench origin along the various wedge and spacers transitions in the lead end of the magnet. We present results on the identified quench locations for the second and third thermal cycle in this paper.**

***Index Terms*— Accelerator magnets, quench, quench propagation, training.**

I. Introduction

THE LARP collaboration and CERN have developed the MQXF series Nb_3Sn quadrupoles (150 mm aperture, 132.6 T/m gradient) for the LHC luminosity upgrade [1]. Among others, several short prototypes with a magnetic length of 1 m were designed [2],[3]. An extensive testing campaign at FNAL for MQXFS1, the first prototype, was conducted to ensure it matches performance expectations [4]-[8]. Three different test cycles with varying axial and azimuthal pre-stress were conducted, testing new quench protection as well as quench training and memory and field quality studies. During these tests, the quench locations in the coils were recorded using voltage taps and a newly developed quench antenna. The goal was to identify potential weak spots in the magnet performance or mechanical design as well as to study the quench training and quench propagation.

A quench antenna is a device to localize quenches non-invasively and to measure their propagation dynamics. The antenna used for MQXFS1 is based on a design presented in [9] and is described in more detail in [10]. A transient in the magnet current induces inductive voltages in a pickup coil nearby.

This work was supported by the U.S. Department of Energy, Office of Science, Office of High Energy Physics, through the US LHC Accelerator Research Program (LARP) and by the High Luminosity LHC project at CERN. The U.S. Government retains and the publisher, by accepting the article for publication, acknowledges that the U.S. Government retains a non-exclusive, paid-up, irrevocable, world-wide license to publish or reproduce the published form of this manuscript, or allow others to do so, for U.S. Government purposes.

T. Strauss, G. Ambrosio, G. Chlachidze and S. Stoynev are with the Fermi National Accelerator Laboratory, Batavia, IL 80510 USA (e-mail: strauss@fnal.gov).

Paolo Ferracin is with CERN, Geneva, CH (e-mail: paolo.ferracin@cern.ch).

M. Marchevsky, G. Sabbi are with Lawrence Berkeley National Laboratory, Berkeley, CA 94720 USA (e-mail: mmarchevskii@lbl.gov).

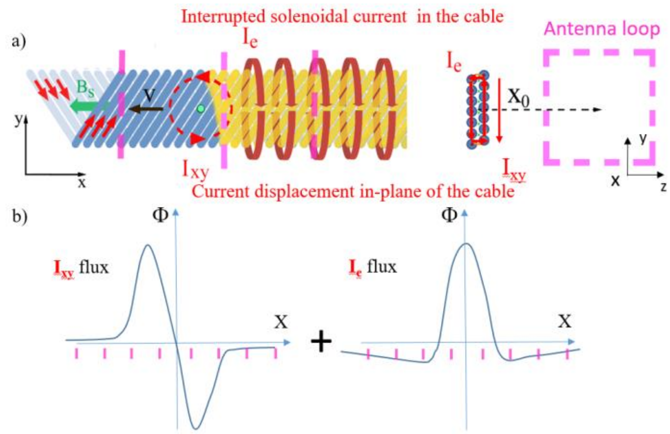

Fig. 1. Adopted from [10] (a). A sketch showing quench propagation in a Rutherford cable. The normal zone expands to the right causing "leakage" of the solenoidal field form the cable interior, as well as current redistribution near the normal zone boundary. Both effects can be simulated as a set of current loops building up along the cable length. When quench front passes along the antenna pickup coil (dashed line) an inductive signal is generated.
(b) Sketches of two possible flux distributions along the antenna axis for a quench at location x=0 (or antenna element 4 and 5), caused by a pure I_{xy} or I_e current component, respectively. In the first milliseconds, the quench is localized and the antenna voltages are proportional to $d\Phi/dt$. Integrating the early rise of the antenna signal should reproduce the flux profile.

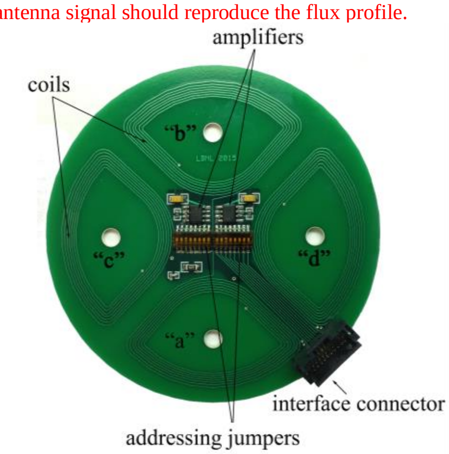

Fig 2. A photograph of the assembled antenna board (single element).

A quench is localized by detecting the gradient of the axial field component in the magnet bore arising from a normal zone formation in the superconducting cable. The antenna consists of two pairs of dipole-bucked pickup coils. Pairs are orthogonal to each other in the sensor's *xy* plane. A warm bore ("anti-cryostat") with 130 mm inner diameter allows to place the antenna in the magnet bore. The antenna location in the warm bore can be adjusted, so varying coverage along the magnet bore (z-axis) is possible. The elements of the quench antenna are separated by spacers to detect time derivatives of the flux change, as indicated in Fig. 1 b).

Fig. 3. a) A photograph of the quench antenna at 107.1 cm length, b) A photograph of the warm top with the clamped quench antenna rod. c) A picture of the shortened quench antenna with 5 segments at 2.54 cm spacing, and three segments with 5.08 cm spacing.

Localization with 20 mm accuracy was presented previously with a fixed spacer length of 15.24 cm (6 “) [10]. In this paper, we show the results from extensive studies with varying spacer lengths and positioning of the antenna around the magnet center and the lead end region of the magnet.

II. Quench Antenna Configurations and Experimental Verification

The antenna was designed such that multiple elements can be stacked to cover different MQXF series magnets with magnetic lengths of 1 m, 4.2 m and 7.15 m. For this test, the antenna was equipped with 8 elements, each made from a 4-layer 0.6 mm thick printed circuit board, and were 95 mm in diameter. Fig. 2 shows each board has two dipole-bucked pair of sectorial 90-degree wide flat coils that rotated by a 180 degree angle (coil pairs are denoted as “ab” and “cd”). The boards are connected by a flat ribbon cable for power supply and signals, a connector box allows to connect the antenna to the FNAL quench data acquisition system. For reduction of parasitic electromagnetic noise in the warm bore due to the magnet test facility, the entire flat ribbon cable is encased by a copper-mesh shield and the coil areas on boards were laminated at one side with a ground-terminated 0.1 mm thick aluminum foil. The fully assembled antenna section is shown in Fig 3 a), using 15.24 cm (6 “) spacers for an antenna length of 107.1 cm. This ensure full length coverage of the MQXFS1 magnet straight section (100.2 cm), with a small overlap to the coil ends. To center the quench antenna, the mechanical center of the magnet was used as shown in Fig. 4. Fig. 3 b) shows how the quench antenna location is fixed to the warm bore. A

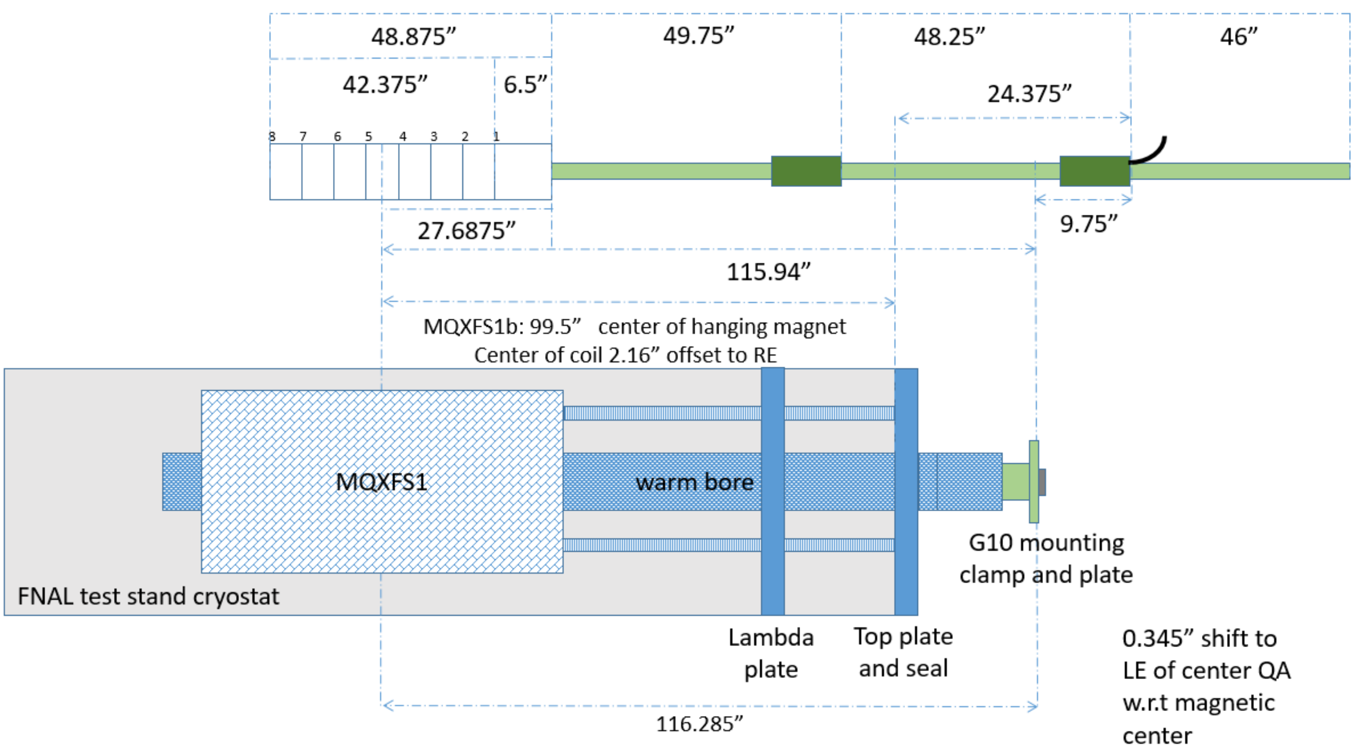

Fig. 4. A schematic of the mechanical quench antenna centering. The magnet inside the FNAL test stand is at a depth of 295.36 cm (116.285 inches) w.r.t the mounting bracket that clamps the quench antenna in place. A comparison with the magnetic center shows a displacement of 0.87 cm (0.345 inches).

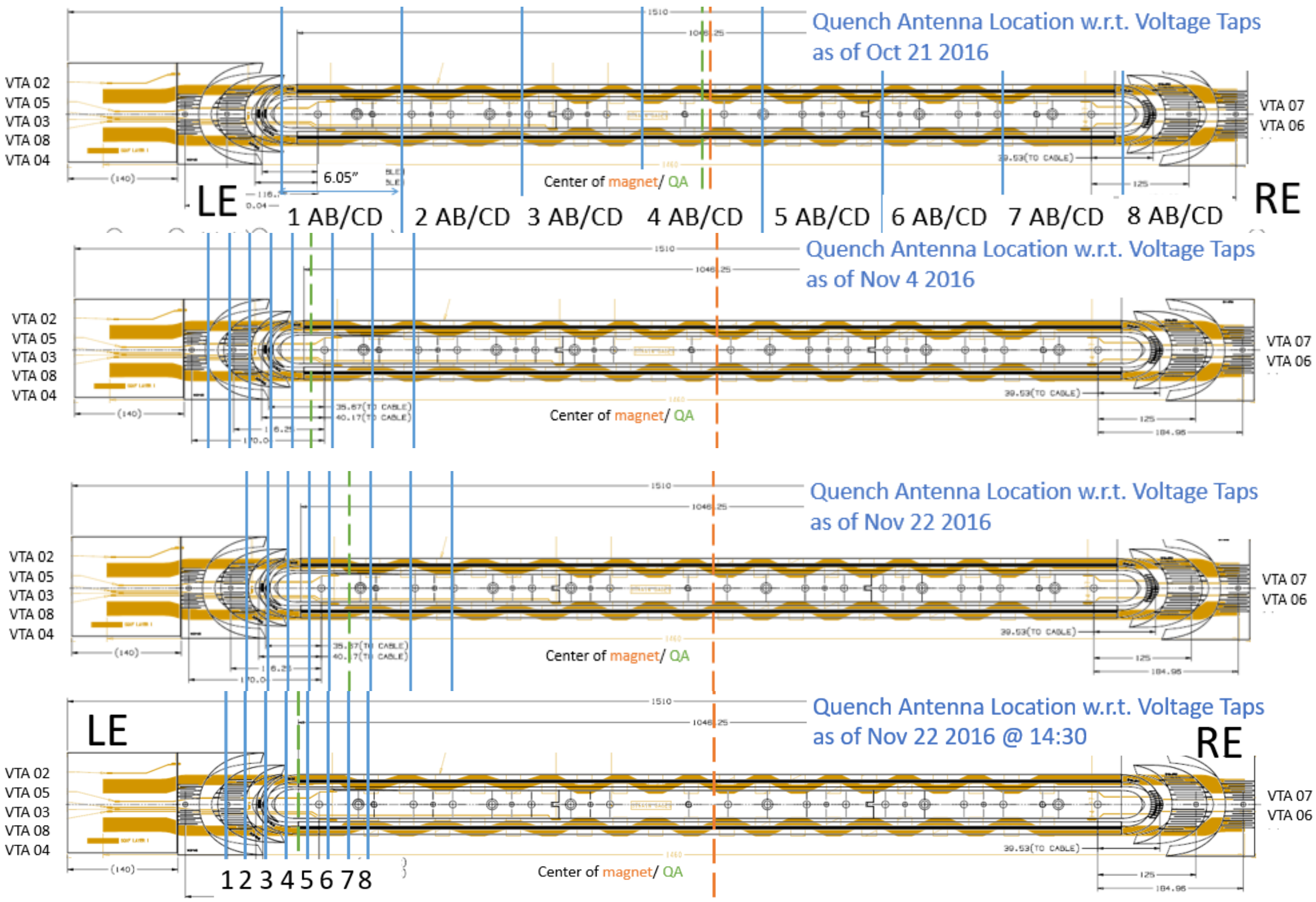

Fig. 5. A schematic of the quench antenna positioning. The segments are represented by full lines, overlaid with the mechanical assembly drawing to indicated the position of each segment along the z-axis. For the top and bottom plot the antenna segments are labeled and lead end (LE) and return end (RE) of the magnet is indicated. The voltage taps locations are labeled for comparison too.

10.16 cm (4 “) tall plastic cone (in blue) is used to guide the magnetic probe and quench antenna into the warm bore. Two G10 half sphere compress on the antenna rod fixing its location along the z-axis. A dry nitrogen vent prevents ice buildup in the bore. A comparison between the mechanical and magnetic center shows a shift of 0.87 cm between the two. For the second test run of the MQXFS1 magnet starting on October 21, the quench location was mostly in the lead end (LE) of the magnet, where only one antenna segment was located. To help further localize the quench location, we decided to reduce the distance between antenna segments, and cover only the LE area. Fig. 5 shows the time evolution of the quench antenna location in the frame of the MQXFS1 magnet. From November 04, we used a shortened quench antenna with 5 segments at 2.54 cm distance, and three segments at 5.08 cm distance each, an image of the shorter antenna is shown in Fig 3 c). After modifying the antenna length, the antenna was placed such that it covered the LE of the MQXFS1 magnet. The quench antenna covered the turns inside and outside of the middle pole spacer. Several quenches at this position were recorded.

Data analyzed during this time indicated that the wedge and end-spacer transition was a possible point of interest for the quench origin. Thus, the antenna location was adjusted again on November 22 to center the 2.54 cm sized spaced quench antenna segments along this transition. The observed signal in the first quench of the day indicated a quench location very close to the first segment’s xy plane, with no observable signals in the 5.08 cm spaced segments. For that reason, we decided to set all segments to a 2.54 cm spacing, move the antenna such that it covered only the LE, with the center of the

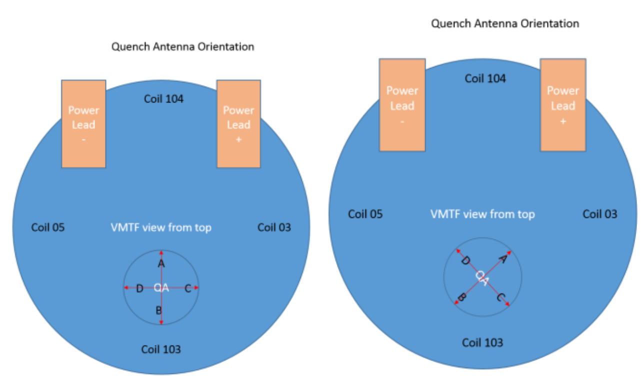

Fig. 6. Orientation of the quench antenna coil w.r.t. to the magnet coil orientation., after a 45 degree shift was suggested to distinguish transition and non-transition side quenches in the coil

antenna at the wedge transition from November 24 in the afternoon. In Fig. 8 we show two examples with voltage tap and quench antenna signals and the analysis process. From the voltage tap reading (dashed lines) we observe that the quench is first seen in the multiturn segment between the first wedge and the pole (segment 03-04 of coil 003). The quench antenna, located in the LE, has bipolar signals for segments 2-7. The integrated flux during the initial voltage rise (2-3 ms) of the quench antenna is shown in the inserts of Fig. 8 a) and b) each. Comparing the pattern with Fig. 1 b) indicates the quench origin around segment #5. To localize the quench origin more precisely, we rotated the quench antenna 45 degrees, such that the dipole-bucks coil segment face parting plane (mid plane) between coils the instead of the pole, as indicated in Fig. 6. The detailed analysis of the data is still pending.

In Fig. 7 we overlay boxes of the various quench locations as indicated by the quench antenna segments. The number in the center associate the quench time (MM/DD HH:MM) and the coil number. The quench antenna segment id (QA #) was converted to the antenna location frame of November 22. The boxes in the image are utilizing information obtained from the voltage taps; they indicated a quench origin near the pole and first wedge transition, where a change in materials could explain quench origins. For two events, the quench location was in the lead end turn. As the LE contains a multiturn segment, a finer localization was not possible, thus the larger rectangular box. The analysis for the third run is pending. Most quenches occurred in coil 03; overlaying the quenches and extending the boxes with a five percent shading creates a quench density map. Most quenches occur on the wedge and pole spacer transition.

Fig. 8 Example quenches with voltage tap and quench antenna signal, both with a similar quench pattern. Quenches occur in the same coil 03. The insert shows the integrated flux during the initial antenna voltage signal rise, used to localize the quench, as explained in the Introduction and Fig 1b).

III. Conclusion

We present the extensively tested and modified quench antenna developed for the MQXF magnet series for localizing quenches in high-field accelerator magnets. Thanks to the 20 mm resolution of the quench antenna and the voltage tap information we were able to identify the axial localization of quenches in the wedge to end-spacer transition area of the coils. While we were not able to distinguish between transition and non-transition side of the coils, the obtained data proved the working principle of the antenna and provided useful input for the future design and assembly of the MQXF magnet series.

Acknowledgment

We are thankful to FNAL magnet test facility personnel and the LBNL technician support is gratefully acknowledged.

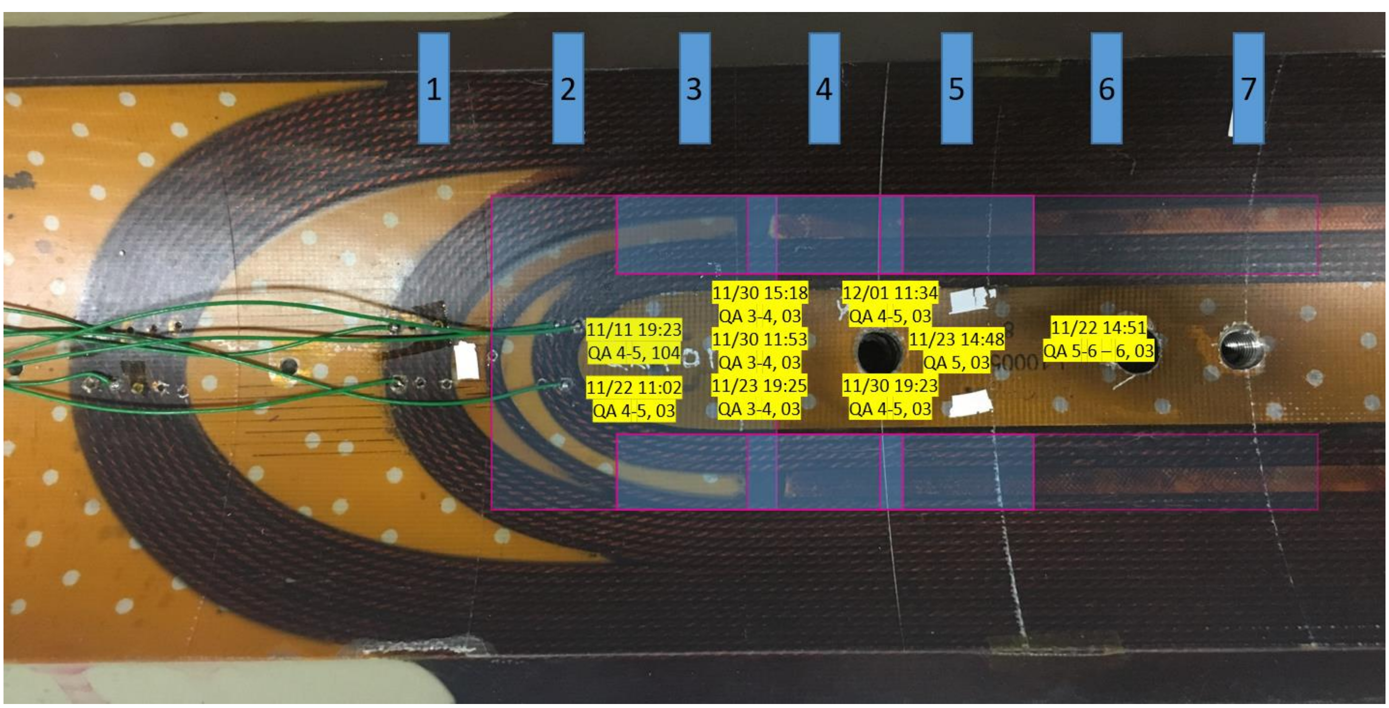

Fig.7. Quench Location in the lead end of the MQXFS1 magnet. Numbers show MM/DD HH:MM, QA # (converted to position in this image), Coil #.

REFERENCES

[1] G. G. Apollinari, I. Béjar Alonso, O. Brüning, M. Lamont, and L. Rossi, "High-Luminosity Large Hadron Collider (HL-LHC): Preliminary Design Report", *CERN Yellow Reports: Monographs*, CERN-2015-005, Available: http://cds.cern.ch/record/2116337

[2] P. Ferracin, G. Ambrosio, M. Anerella, F. Borgnolutti, R. Bossert, D. Cheng, D. R. Dietderich, H. Felice, A. Ghosh, A. Godeke, S. Izquierdo Bermudez, P. Fessia, S. Krave, M. Juchno, J. C. Perez, L. Oberli, G. Sabbi, E. Todesco, and M. Yu, "Magnet design of the 150 mm aperture low-quadrupoles for the High Luminosity LHC", *IEEE Trans. Appl. Supercond.*, vol. 24, no. 3, 2014, Art. no. 4002306.

[3] G. Ambrosio, "Nb_3Sn high field magnets for the High Luminosity LHC upgrade project", *IEEE Trans. Appl. Supercond.*, vol. 25, no. 3, 2015, Art. no. 4002107.

[4] J. DiMarco, G. Ambrosio, G. Chlachidze, P. Ferracin, E. Holik, G. Sabbi, S. Stoynev, T. Strauss, C. Sylvester, M. Tartaglia, E. Todesco, G. Velev, X. Wang, "Magnetic Measurements of the First Nb_3Sn Model Quadrupole (MQXFS) for the High-Luminosity LHC", *IEEE Trans. Appl. Supercond.*, vol. 27, no. 4, 2017, Art. no. 9000105.

[5] G. Chlachidze **,** G. Ambrosio**,** M. Anerella**,** R. Bossert**,** E. Cavanna**,** D. Cheng**,** D. Dietderich**,** J. DiMarco**,** H. Felice**,** P. Ferracin**,** A. Ghosh**,** P. Grosclaude**,** M. Guinchard**,** A.R. Hafalia**,** E. Holik**,** S. Izquierdo Bermudez**,** S. Krave**,** M. Marchevsky**,** F. Nobrega**,** D. Orris**,** H. Pan**,** J. C. Perez**,** S. Prestemon**,** E. Ravaioli**,** G.L. Sabbi**,** T. Salmi**,** J. Schmalzle**,** S. Stoynev**,** T. Strauss**,** C. Sylvester**,** M. Tartaglia**,** E. Todesco**,** G. Vallone**,** G. Velev**,** P. Wanderer**,** X. Wang**,** M. Yu, "Performance of the first short model 150 mm aperture Nb_3Sn Quadrupole MQXFS for the High-Luminosity LHC upgrade", *IEEE Trans. Appl. Supercond.*, vol. 27, no. 4, 2017, Art. no. 4000205.

[6] G. Vallone, G. Ambrosio, E. Anderssen, N. Bourcey, D. Cheng, H. Felice, P. Ferracin, C. Fichera, P. Grosclaude, M. Guinchard, M. Juchno, H. Pan, J. Carlos Perez, S. Prestemon, "Mechanical Performance of Short Models for MQXF, the Nb3Sn Low-β Quadrupole for the Hi-Lumi LHC", *IEEE Trans. Appl. Supercond.*, vol. 27, no. 4, 2017, Art. no. 4002906.

[7] S. Stoynev, et al., "Summary of test results of MQXFS1 - the first short model 150 mm aperture Nb3Sn quadrupole for the High-Luminosity LHC upgrade", *IEEE Trans. Appl. Supercond.*, submitted for publication.

[8] S. Izquierdo Bermudez, et al., "Geometric field errors of Short Models for MQXF, the Nb3Sn low-beta Quadrupole for the High Luminosity LHC", *IEEE Trans. Appl. Supercond.*, submitted for publication.

[9] M. Marchevsky, J. DiMarco, H. Felice, A. R. Hafalia, J. Joseph; J. Lizarazo, X. Wang; G. Sabbi., "Magnetic detection of quenches in high-field accelerator magnets", *IEEE Trans. Appl. Supercond.*, vol. 23, no. 3, 2013, Art. no. 9001005.

[10] M. Marchevsky, G. Sabbi, S. Prestemon, T. Strauss, S. Stoynev, G. Chlachidze, "Magnetic Quench Antenna for MQXF Quadrupoles", *IEEE Trans. Appl. Supercond.*, vol. 27, no. 4, 2017, Art. no. 9000505.